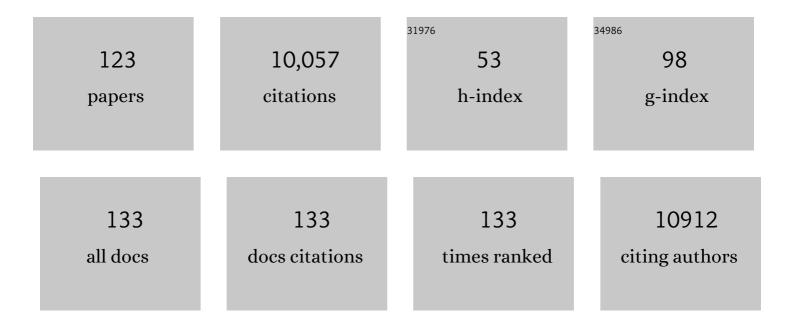
Wilson A Smith

List of Publications by Year in descending order

Source: https://exaly.com/author-pdf/1320527/publications.pdf Version: 2024-02-01



#	Article	IF	CITATIONS
1	The effect of catholyte and catalyst layer binders on CO2 electroreduction selectivity. Chem Catalysis, 2022, 2, 400-421.	6.1	9
2	Polymer Modification of Surface Electronic Properties of Electrocatalysts. ACS Energy Letters, 2022, 7, 1586-1593.	17.4	13
3	An economic analysis of the role of materials, system engineering, and performance in electrochemical carbon dioxide conversion to formate. Journal of Cleaner Production, 2022, 351, 131564.	9.3	7
4	High Indirect Energy Consumption in AEM-Based CO ₂ Electrolyzers Demonstrates the Potential of Bipolar Membranes. ACS Applied Materials & Interfaces, 2022, 14, 557-563.	8.0	18
5	Overcoming Nitrogen Reduction to Ammonia Detection Challenges: The Case for Leapfrogging to Gas Diffusion Electrode Platforms. ACS Catalysis, 2022, 12, 5726-5735.	11.2	24
6	Modeling the Local Environment within Porous Electrode during Electrochemical Reduction of Bicarbonate. Industrial & Engineering Chemistry Research, 2022, 61, 10461-10473.	3.7	25
7	Characterizing CO ₂ Reduction Catalysts on Gas Diffusion Electrodes: Comparing Activity, Selectivity, and Stability of Transition Metal Catalysts. ACS Applied Energy Materials, 2022, 5, 5983-5994.	5.1	23
8	(Invited) Experimental Measurement of Spatial Activity on CO ₂ & CO Reduction Gas Diffusion Electrodes. ECS Meeting Abstracts, 2022, MA2022-01, 1775-1775.	0.0	0
9	Role of the Carbon-Based Gas Diffusion Layer on Flooding in a Gas Diffusion Electrode Cell for Electrochemical CO ₂ Reduction. ACS Energy Letters, 2021, 6, 33-40.	17.4	221
10	Orientation of a bipolar membrane determines the dominant ion and carbonic species transport in membrane electrode assemblies for CO ₂ reduction. Journal of Materials Chemistry A, 2021, 9, 11179-11186.	10.3	40
11	Accelerating ¹ H NMR Detection of Aqueous Ammonia. ACS Omega, 2021, 6, 5698-5704.	3.5	16
12	Operando Topography and Mechanical Property Mapping of CO ₂ Reduction Gas-Diffusion Electrodes Operating at High Current Densities. Journal of the Electrochemical Society, 2021, 168, 044505.	2.9	9
13	Water and Solute Activities Regulate CO ₂ Reduction in Gas-Diffusion Electrodes. Journal of Physical Chemistry C, 2021, 125, 13085-13095.	3.1	15
14	Introducing special issue on photocatalysis and photoelectrochemistry. Journal of Chemical Physics, 2021, 154, 190401.	3.0	0
15	Emerging collaborations at the forefront of growth in electrochemical synthesis. IScience, 2021, 24, 102639.	4.1	0
16	Insights and Challenges for Applying Bipolar Membranes in Advanced Electrochemical Energy Systems. ACS Energy Letters, 2021, 6, 2539-2548.	17.4	86
17	Process modeling, techno-economic assessment, and life cycle assessment of the electrochemical reduction of CO2: a review. IScience, 2021, 24, 102813.	4.1	59
18	Along the Channel Gradients Impact on the Spatioactivity of Gas Diffusion Electrodes at High Conversions during CO ₂ Electroreduction. ACS Sustainable Chemistry and Engineering, 2021, 9, 1286-1296.	6.7	47

#	Article	IF	CITATIONS
19	Assessing Silver Palladium Alloys for Electrochemical CO ₂ Reduction in Membrane Electrode Assemblies. ChemElectroChem, 2021, 8, 4515-4521.	3.4	4
20	Operando Infrared Spectroscopy Reveals the Dynamic Nature of Semiconductor–Electrolyte Interface in Multinary Metal Oxide Photoelectrodes. Journal of the American Chemical Society, 2021, 143, 18581-18591.	13.7	28
21	Cation-Driven Increases of CO ₂ Utilization in a Bipolar Membrane Electrode Assembly for CO ₂ Electrolysis. ACS Energy Letters, 2021, 6, 4291-4298.	17.4	88
22	Liquid–Solid Boundaries Dominate Activity of CO ₂ Reduction on Gas-Diffusion Electrodes. ACS Catalysis, 2020, 10, 14093-14106.	11.2	114
23	Copper and silver gas diffusion electrodes performing CO ₂ reduction studied through <i>operando</i> X-ray absorption spectroscopy. Catalysis Science and Technology, 2020, 10, 5870-5885.	4.1	13
24	High-Performance Bipolar Membrane Development for Improved Water Dissociation. ACS Applied Polymer Materials, 2020, 2, 4559-4569.	4.4	45
25	Reduced Ion Crossover in Bipolar Membrane Electrolysis <i>via</i> Increased Current Density, Molecular Size, and Valence. ACS Applied Energy Materials, 2020, 3, 5804-5812.	5.1	45
26	A Robust, Scalable Platform for the Electrochemical Conversion of CO ₂ to Formate: Identifying Pathways to Higher Energy Efficiencies. ACS Energy Letters, 2020, 5, 1825-1833.	17.4	126
27	Competition and selectivity during parallel evolution of bromine, chlorine and oxygen on IrOx electrodes. Journal of Catalysis, 2020, 389, 99-110.	6.2	21
28	In Situ ATR–SEIRAS of Carbon Dioxide Reduction at a Plasmonic Silver Cathode. Journal of the American Chemical Society, 2020, 142, 11750-11762.	13.7	68
29	Electrochemical CO ₂ Reduction Over Bimetallic Au–Sn Thin Films: Comparing Activity and Selectivity against Morphological, Compositional, and Electronic Differences. Journal of Physical Chemistry C, 2020, 124, 14573-14580.	3.1	9
30	Hidden figures of photo-charging: a thermo-electrochemical approach for a solar-rechargeable redox flow cell system. Sustainable Energy and Fuels, 2020, 4, 2650-2655.	4.9	8
31	Facet-Dependent Selectivity of Cu Catalysts in Electrochemical CO ₂ Reduction at Commercially Viable Current Densities. ACS Catalysis, 2020, 10, 4854-4862.	11.2	331
32	Tailored energy level alignment at MoOX/GaP interface for solar-driven redox flow battery application. Journal of Chemical Physics, 2020, 152, 124710.	3.0	7
33	Electrochemical CO ₂ reduction on nanostructured metal electrodes: fact or defect?. Chemical Science, 2020, 11, 1738-1749.	7.4	83
34	Competition and Interhalogen Formation During Parallel Electrocatalytic Oxidation of Bromide and Chloride on Pt. Journal of the Electrochemical Society, 2020, 167, 046505.	2.9	10
35	Design principles for efficient photoelectrodes in solar rechargeable redox flow cell applications. Communications Materials, 2020, 1, .	6.9	14
36	How Local Reaction and Process Conditions Influence CO2 Reduction to Multicarbon Products on Copper Gas-Diffusion Electrodes. ECS Meeting Abstracts, 2020, MA2020-01, 1515-1515.	0.0	0

#	Article	IF	CITATIONS
37	Pathways to Industrial-Scale Fuel Out of Thin Air from CO2 Electrolysis. Joule, 2019, 3, 1822-1834.	24.0	137
38	Electrochemical impedance spectroscopy as a performance indicator of water dissociation in bipolar membranes. Journal of Materials Chemistry A, 2019, 7, 19060-19069.	10.3	45
39	Unravelling the practical solar charging performance limits of redox flow batteries based on a single photon device system. Sustainable Energy and Fuels, 2019, 3, 2399-2408.	4.9	15
40	Chemisorption of Anionic Species from the Electrolyte Alters the Surface Electronic Structure and Composition of Photocharged BiVO ₄ . Chemistry of Materials, 2019, 31, 7453-7462.	6.7	30
41	Maximizing Ag Utilization in High-Rate CO ₂ Electrochemical Reduction with a Coordination Polymer-Mediated Gas Diffusion Electrode. ACS Energy Letters, 2019, 4, 2024-2031.	17.4	85
42	Inâ€Situ Infrared Spectroscopy Applied to the Study of the Electrocatalytic Reduction of CO ₂ : Theory, Practice and Challenges. ChemPhysChem, 2019, 20, 2904-2925.	2.1	66
43	In Situ Infrared Spectroscopy Reveals Persistent Alkalinity near Electrode Surfaces during CO ₂ Electroreduction. Journal of the American Chemical Society, 2019, 141, 15891-15900.	13.7	191
44	CO ₂ reduction on gas-diffusion electrodes and why catalytic performance must be assessed at commercially-relevant conditions. Energy and Environmental Science, 2019, 12, 1442-1453.	30.8	692
45	Light induced formation of a surface heterojunction in photocharged CuWO ₄ photoanodes. Faraday Discussions, 2019, 215, 175-191.	3.2	7
46	Hydrocarbon Synthesis via Photoenzymatic Decarboxylation of Carboxylic Acids. Journal of the American Chemical Society, 2019, 141, 3116-3120.	13.7	123
47	<i>Operando</i> EXAFS study reveals presence of oxygen in oxide-derived silver catalysts for electrochemical CO ₂ reduction. Journal of Materials Chemistry A, 2019, 7, 2597-2607.	10.3	125
48	Beyond artificial photosynthesis: general discussion. Faraday Discussions, 2019, 215, 422-438.	3.2	0
49	Demonstrator devices for artificial photosynthesis: general discussion. Faraday Discussions, 2019, 215, 345-363.	3.2	2
50	Synthetic approaches to artificial photosynthesis: general discussion. Faraday Discussions, 2019, 215, 242-281.	3.2	5
51	Suppressing H ₂ Evolution and Promoting Selective CO ₂ Electroreduction to CO at Low Overpotentials by Alloying Au with Pd. ACS Catalysis, 2019, 9, 3527-3536.	11.2	79
52	Electronic Effects Determine the Selectivity of Planar Au–Cu Bimetallic Thin Films for Electrochemical CO ₂ Reduction. ACS Applied Materials & Interfaces, 2019, 11, 16546-16555.	8.0	71
53	Introductory Guide to Assembling and Operating Gas Diffusion Electrodes for Electrochemical CO ₂ Reduction. ACS Energy Letters, 2019, 4, 639-643.	17.4	158
54	Modeling the electrical double layer to understand the reaction environment in a CO ₂ electrocatalytic system. Energy and Environmental Science, 2019, 12, 3380-3389.	30.8	125

#	Article	IF	CITATIONS
55	Designing a hybrid thinâ€film/wafer silicon triple photovoltaic junction for solar water splitting. Progress in Photovoltaics: Research and Applications, 2019, 27, 245-254.	8.1	10
56	Lateral Adsorbate Interactions Inhibit HCOO ^{â^'} while Promoting CO Selectivity for CO ₂ Electrocatalysis on Silver. Angewandte Chemie - International Edition, 2019, 58, 1345-1349.	13.8	93
57	Lateral Adsorbate Interactions Inhibit HCOO ^{â^'} while Promoting CO Selectivity for CO ₂ Electrocatalysis on Silver. Angewandte Chemie, 2019, 131, 1359-1363.	2.0	25
58	Rücktitelbild: Lateral Adsorbate Interactions Inhibit HCOO ^{â^'} while Promoting CO Selectivity for CO ₂ Electrocatalysis on Silver (Angew. Chem. 5/2019). Angewandte Chemie, 2019, 131, 1534-1534.	2.0	0
59	General Considerations for Improving Photovoltage in Metal–Insulator–Semiconductor Photoanodes. Journal of Physical Chemistry C, 2018, 122, 5462-5471.	3.1	54
60	Au Dendrite Electrocatalysts for CO ₂ Electrolysis. Journal of Physical Chemistry C, 2018, 122, 10006-10016.	3.1	30
61	Improving the Back Surface Field on an Amorphous Silicon Carbide Thinâ€Film Photocathode for Solar Water Splitting. ChemSusChem, 2018, 11, 1797-1804.	6.8	6
62	Emerging Postsynthetic Improvements of BiVO ₄ Photoanodes for Solar Water Splitting. ACS Energy Letters, 2018, 3, 112-124.	17.4	97
63	Solar Redox Flow Batteries with Organic Redox Couples in Aqueous Electrolytes: A Minireview. Journal of Physical Chemistry C, 2018, 122, 25729-25740.	3.1	42
64	In Situ Fabrication and Reactivation of Highly Selective and Stable Ag Catalysts for Electrochemical CO ₂ Conversion. ACS Energy Letters, 2018, 3, 1301-1306.	17.4	136
65	Ion transport mechanisms in bipolar membranes for (photo)electrochemical water splitting. Sustainable Energy and Fuels, 2018, 2, 2006-2015.	4.9	97
66	Pathways to electrochemical solar-hydrogen technologies. Energy and Environmental Science, 2018, 11, 2768-2783.	30.8	238
67	Treatment of Organic Pollutants Using a Solar Energy Driven Photoâ€Oxidation Device. Advanced Sustainable Systems, 2017, 1, 1700010.	5.3	2
68	Near-complete suppression of surface losses and total internal quantum efficiency in BiVO ₄ photoanodes. Energy and Environmental Science, 2017, 10, 1517-1529.	30.8	159
69	Hot Carrier Generation and Extraction of Plasmonic Alloy Nanoparticles. ACS Photonics, 2017, 4, 1146-1152.	6.6	97
70	Probing the Reaction Mechanism of CO ₂ Electroreduction over Ag Films via Operando Infrared Spectroscopy. ACS Catalysis, 2017, 7, 606-612.	11.2	327
71	Electrochemical reduction of CO2 on compositionally variant Au-Pt bimetallic thin films. Nano Energy, 2017, 42, 51-57.	16.0	99
72	Interfacial engineering of metal-insulator-semiconductor junctions for efficient and stable photoelectrochemical water oxidation. Nature Communications, 2017, 8, 15968.	12.8	177

#	Article	IF	CITATIONS
73	Solar fuel production by using PV/PEC junctions based on earth-abundant materials. , 2017, , .		0
74	Nanostructured Catalysts for the Electrochemical Reduction of CO2. Nanostructure Science and Technology, 2017, , 337-373.	0.1	4
75	The Role of Size and Dimerization of Decorating Plasmonic Silver Nanoparticles on the Photoelectrochemical Solar Water Splitting Performance of BiVO ₄ Photoanodes. ChemNanoMat, 2016, 2, 739-747.	2.8	33
76	Bipolar Membraneâ€Assisted Solar Water Splitting in Optimal pH. Advanced Energy Materials, 2016, 6, 1600100.	19.5	156
77	Controllable Hydrocarbon Formation from the Electrochemical Reduction of CO ₂ over Cu Nanowire Arrays. Angewandte Chemie - International Edition, 2016, 55, 6680-6684.	13.8	471
78	Photoelectrocatalytic oxidation of phenol for water treatment using a BiVO ₄ thin-film photoanode. Journal of Materials Research, 2016, 31, 2627-2639.	2.6	14
79	Solar fuel production by using PV/PEC junctions based on earth-abundant materials. , 2016, , .		1
80	A thin-film silicon/silicon hetero-junction hybrid solar cell for photoelectrochemical water-reduction applications. Solar Energy Materials and Solar Cells, 2016, 150, 82-87.	6.2	17
81	Photoelectrochemical Cell Design, Efficiency, Definitions, Standards, and Protocols. , 2016, , 163-197.		10
82	Plasmonic nanoparticle-semiconductor composites for efficient solar water splitting. Journal of Materials Chemistry A, 2016, 4, 17891-17912.	10.3	165
83	Selective and Efficient Reduction of Carbon Dioxide to Carbon Monoxide on Oxideâ€Derived Nanostructured Silver Electrocatalysts. Angewandte Chemie, 2016, 128, 9900-9904.	2.0	117
84	Selective and Efficient Reduction of Carbon Dioxide to Carbon Monoxide on Oxideâ€Derived Nanostructured Silver Electrocatalysts. Angewandte Chemie - International Edition, 2016, 55, 9748-9752.	13.8	422
85	Efficient Electrochemical Production of Syngas from CO ₂ and H ₂ O by using a Nanostructured Ag/g ₃ N ₄ Catalyst. ChemElectroChem, 2016, 3, 1497-1502.	3.4	46
86	Special issue on recent advances in energy storage and conversion devices. Chemical Engineering Science, 2016, 154, 1-2.	3.8	1
87	Synergistic Electrochemical CO ₂ Reduction and Water Oxidation with a Bipolar Membrane. ACS Energy Letters, 2016, 1, 1143-1148.	17.4	134
88	Photoelectrochemical water splitting with porous α-Fe2O3 thin films prepared from Fe/Fe-oxide nanoparticles. Applied Catalysis A: General, 2016, 523, 130-138.	4.3	35
89	Controllable Hydrocarbon Formation from the Electrochemical Reduction of CO ₂ over Cu Nanowire Arrays. Angewandte Chemie, 2016, 128, 6792-6796.	2.0	112
90	Engineering the kinetics and interfacial energetics of Ni/Ni–Mo catalyzed amorphous silicon carbide photocathodes in alkaline media. Journal of Materials Chemistry A, 2016, 4, 6842-6852.	10.3	34

#	Article	IF	CITATIONS
91	Photocharged BiVO ₄ photoanodes for improved solar water splitting. Journal of Materials Chemistry A, 2016, 4, 2919-2926.	10.3	203
92	Gradient dopant profiling and spectral utilization of monolithic thin-film silicon photoelectrochemical tandem devices for solar water splitting. Journal of Materials Chemistry A, 2015, 3, 4155-4162.	10.3	35
93	In Situ Observation of Active Oxygen Species in Fe-Containing Ni-Based Oxygen Evolution Catalysts: The Effect of pH on Electrochemical Activity. Journal of the American Chemical Society, 2015, 137, 15112-15121.	13.7	459
94	Semiconducting properties of spinel tin nitride and other IV ₃ N ₄ polymorphs. Journal of Materials Chemistry C, 2015, 3, 1389-1396.	5.5	49
95	Improved charge separation via Fe-doping of copper tungstate photoanodes. Physical Chemistry Chemical Physics, 2015, 17, 9857-9866.	2.8	81
96	Solar Water Splitting Combining a BiVO ₄ Light Absorber with a Ru-Based Molecular Cocatalyst. Journal of Physical Chemistry C, 2015, 119, 7275-7281.	3.1	75
97	Selective electrochemical reduction of CO ₂ to CO on CuO-derived Cu nanowires. Physical Chemistry Chemical Physics, 2015, 17, 20861-20867.	2.8	159
98	Extracting large photovoltages from a-SiC photocathodes with an amorphous TiO ₂ front surface field layer for solar hydrogen evolution. Energy and Environmental Science, 2015, 8, 1585-1593.	30.8	74
99	Oxynitrogenography: Controlled Synthesis of Single-Phase Tantalum Oxynitride Photoabsorbers. Chemistry of Materials, 2015, 27, 7091-7099.	6.7	59
100	Interfacial band-edge energetics for solar fuels production. Energy and Environmental Science, 2015, 8, 2851-2862.	30.8	163
101	Photo-assisted water splitting with bipolar membrane induced pH gradients for practical solar fuel devices. Journal of Materials Chemistry A, 2015, 3, 19556-19562.	10.3	104
102	Investigation of Terahertz Emission from BiVO4/Au Thin Film Interface. Journal of Infrared, Millimeter, and Terahertz Waves, 2015, 36, 1033-1042.	2.2	3
103	Enhancement of the Photoelectrochemical Performance of CuWO ₄ Thin Films for Solar Water Splitting by Plasmonic Nanoparticle Functionalization. Journal of Physical Chemistry C, 2015, 119, 2096-2104.	3.1	90
104	Control of the visible and UV light water splitting and photocatalysis of nitrogen doped TiO2 thin films deposited by reactive magnetron sputtering. Applied Catalysis B: Environmental, 2014, 144, 12-21.	20.2	59
105	A novel approach for the preparation of textured CuO thin films from electrodeposited CuCl and CuBr. Journal of Electroanalytical Chemistry, 2014, 717-718, 243-249.	3.8	37
106	Effect of total gas pressure and O2/N2 flow rate on the nanostructure of N-doped TiO2 thin films deposited by reactive sputtering. Thin Solid Films, 2014, 552, 10-17.	1.8	17
107	Control of the optical and crystalline properties of TiO2 in visible-light active TiO2/TiN bi-layer thin-film stacks. Journal of Applied Physics, 2012, 111, .	2.5	11
108	Fabricating a reactive surface on the fibroin film by a room-temperature plasma jet array for biomolecule immobilization. Chinese Physics B, 2012, 21, 105201.	1.4	6

#	Article	IF	CITATIONS
109	Visible Light Water Splitting via Oxidized TiN Thin Films. Journal of Physical Chemistry C, 2012, 116, 15855-15866.	3.1	19
110	Quasi-core-shell TiO2/WO3 and WO3/TiO2 nanorod arrays fabricated by glancing angle deposition for solar water splitting. Journal of Materials Chemistry, 2011, 21, 10792.	6.7	127
111	Acrylic Acid Polymer Coatings on Silk Fibers by Roomâ€ŧemperature APGD Plasma Jets. Plasma Processes and Polymers, 2011, 8, 701-708.	3.0	42
112	The effect of Ag nanoparticle loading on the photocatalytic activity of TiO2 nanorod arrays. Chemical Physics Letters, 2010, 485, 171-175.	2.6	68
113	Hetero-structured nano-photocatalysts fabricated by dynamic shadowing growth. Proceedings of SPIE, 2010, , .	0.8	1
114	Photoelectrochemical Study of Nanostructured ZnO Thin Films for Hydrogen Generation from Water Splitting. Advanced Functional Materials, 2009, 19, 1849-1856.	14.9	436
115	Photoelectrochemical Water Splitting Using Dense and Aligned TiO ₂ Nanorod Arrays. Small, 2009, 5, 104-111.	10.0	380
116	Measuring the optical properties of a trapped ZnO tetrapod. Microelectronics Journal, 2009, 40, 520-522.	2.0	0
117	The scaling of the photocatalytic decay rate with the length of aligned TiO2 nanorod arrays. Chemical Physics Letters, 2009, 479, 270-273.	2.6	16
118	Superior photocatalytic performance by vertically aligned core–shell TiO2/WO3 nanorod arrays. Catalysis Communications, 2009, 10, 1117-1121.	3.3	83
119	Enhanced Photocatalytic Activity by Aligned WO ₃ /TiO ₂ Two-Layer Nanorod Arrays. Journal of Physical Chemistry C, 2008, 112, 19635-19641.	3.1	84
120	An electrodynamically confined single ZnO tetrapod laser. Applied Physics Letters, 2008, 93, 121102.	3.3	22
121	Structural and optical characterization of WO3 nanorods/films prepared by oblique angle deposition. Journal of Vacuum Science & Technology B, 2007, 25, 1875-1881.	1.3	44
122	Electrochemical AFM techniques to understand cathode topography and electrolyte solvent and solute activities. , 0, , .		0
123	The Influence of Along-the-Channel Gradients on Spatioactivitiy and Spatioselectivity of Gas Diffusion Electrodes during Electrochemical CO2 Reduction. , 0, , .		0